Sensors and Materials, Vol. 37, No. 2 (2025) 475–480
MYU Tokyo

S & M 3922

Dosimetric Properties of Dy-doped Li_2O–B_2O_3 Glasses

Takumi Kato,* Akihiro Nishikawa, Daisuke Nakauchi,
Noriaki Kawaguchi, and Takayuki Yanagida

Nara Institute of Science and Technology (NAIST), 8916-5, Takayama-cho, Ikoma-shi, Nara 630-0192, Japan

(Received October 31, 2024; accepted December 16, 2024)

Keywords: dosimeter, glass, TSL

As dosimetric materials, undoped and Dy-doped 33.3LiO–66.7B_2O_3 glasses were synthesized by the melt-quenching method. Their photoluminescence and thermally stimulated luminescence spectra showed several emission lines. A broad glow peak was observed at ~75 °C in the Dy-doped samples, while the undoped sample showed no glow peaks. A linear relationship between irradiation dose and thermally stimulated luminescence intensity was confirmed from 1 to 1000 mGy when the 0.5% Dy-doped glass was exposed to different doses of X-ray radiation.

1. Introduction

Certain storage-type phosphors have the ability to capture and retain ionizing radiation energy as carriers that are trapped at lattice defects and impurities. When an external treatment is applied, absorbed energy is released, resulting in the release of photons from the materials. In this process, photons are separated into those having thermally stimulated luminosity (TSL),[1–3] optically stimulated luminosity (OSL),[4–6] and radio-photoluminescence (RPL),[7–9] depending on the emission mechanism. They are utilized in many different applications, including personal dosimeters and medical imaging, because the quantity of low-energy photons released by external treatment is proportional to the amount of ionizing radiation. Storage phosphors with such a memorization function of ionizing radiation are collectively called dosimetric materials. Numerous types of dosimetric materials have been studied and brought to market thus far, and research is still being done to find new high-performing dosimetric materials. It is necessary for novel dosimetric materials to have higher luminescence intensity, wider dynamic range, and less fading. In particular, their effective atomic number (Z_{eff}) should be close to that of human soft tissues when used for personal dosimeters.

Therefore, host materials composed of Li and B can be promising candidates for dosimetric materials. Actually, Mn-doped $Li_2B_4O_7$ crystals, with a chemical composition close to human soft tissue, have been commercialized as TLD-800.[10,11] In addition, Li_2O–B_2O_3 glasses doped with luminescence centers have been reported as dosimetric materials.[12–17] However, most reports focused on transition metals such as Mn, Ag, and

*Corresponding author: e-mail: kato.takumi.ki5@ms.naist.jp
https://doi.org/10.18494/SAM5424

ISSN 0914-4935
https://myukk.org/

Cu as luminescence centers. In this study, we prepared Li_2O–B_2O_3 glasses doped with Dy as a rare-earth element and investigated their optical and dosimetric properties. Owing to the high luminescence intensity produced by the 4f–4f transitions of the Dy^{3+} ion, Dy^{3+} is frequently used as a dopant ion for many phosphor applications.[18] Previous research has shown the applicability of numerous Dy-doped phosphors including Dy-doped CaF_2, which is used in commercial dosimeters (Thermo Fisher Scientific, TLD-200).[19]

2. Materials and Methods

$33.3Li_2O$-$66.7B_2O_3$-xDy_2O_3 (x = 0, 0.1, 0.5, 1.0, 3.0, and 5.0 mol%) glasses were fabricated by the conventional melt-quenching method. Li_2CO_3, B_2O_3, and Dy_2O_3 (4N) were mixed and melted in an alumina crucible in an electric furnace at 1000 ℃ for 1 h under ambient atmosphere. Following the synthesis, each sample was polished to a thickness of 1 mm with a polishing machine (MetaServ 250, Buehler), and its transmittance and X-ray diffraction (XRD) patterns were evaluated using a JASCO V670 spectrometer and MiniFlex 600 (RIGAKU), respectively. The photoluminescence (PL) excitation and emission contour graph and the PL quantum yield (QY) were measured using a Quantaurus-QY spectrometer (Hamamatsu). PL decay times were recorded using a Quantaurus-τ instrument by selecting the excitation and monitored wavelengths from the contour graph. TSL glow curves and spectra were measured as dosimetric characteristics. A photon-counting head (H11890-01, Hamamatsu) recorded TSL glow curves at 30–400 ℃ when the samples were heated by a temperature controller/power supply (SCR-SHQ-A, SAKAGUCHIE.H VOC) at a heating rate of 1 ℃/s. As the radiation source, an X-ray generator (XRBOP&N200X4550, Spellman) was employed. A CCD-based spectrometer (QE Pro, Ocean Optics) was used to measure a TSL spectrum.[20]

3. Results and Discussion

The appearance of each sample under room light and UV light with a wavelength of 365 nm is shown in Fig. 1. The prepared samples were processed to 8 × 8 × 1.0 mm^3. The Z_{eff} of the samples changed from 7.3, 11.3, 16.9, 20.3, and 27.4 to 31.4 as the Dy concentration increased from 0, 0.1, 0.5, 1.0, and 3.0 to 5.0%. All samples had transparency, and the 5.0% Dy-doped sample was colored yellow. Under UV light, the Dy-doped samples showed yellowish-white luminescence. For XRD examination, some of the samples were ground into powder. The XRD patterns of the glass samples are shown in Fig. 2. There was only one broad peak, centered at 25 degrees, in all the samples. This broad peak has been referred to as a halo peak, which is indicative of amorphous materials,[21,22] and the outcome implied that no crystallization occurred in the samples.

Figure 3 shows the in-line transmittance spectra of the Dy-doped glasses. All the Li_2O–B_2O_3 glasses had ~80% transmittance in a wavelength range without an absorption band. An absorption band was observed at 280 nm in common with undoped and Dy-doped samples; thus, this absorption should be due to the host material. Some absorption lines due to Dy^{3+} 4f–4f transitions were detected at a wavelength longer than 300 nm. Typical electron transitions due to Dy^{3+} corresponding to each absorption line are shown in Fig. 3.[23,24]

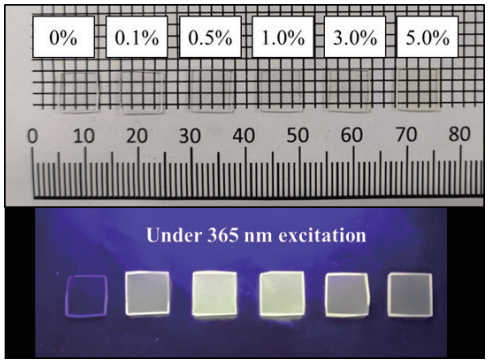

Fig. 1. (Color online) Appearances of Dy-doped Li_2O-B_2O_3 samples.

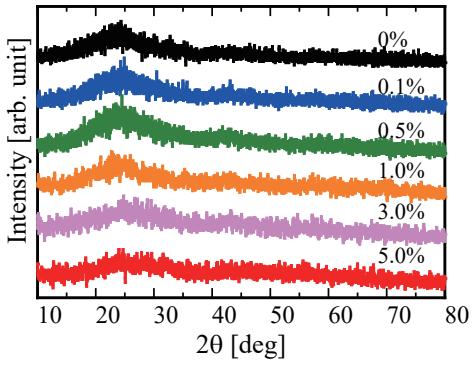

Fig. 2. (Color online) XRD patterns of the glass samples.

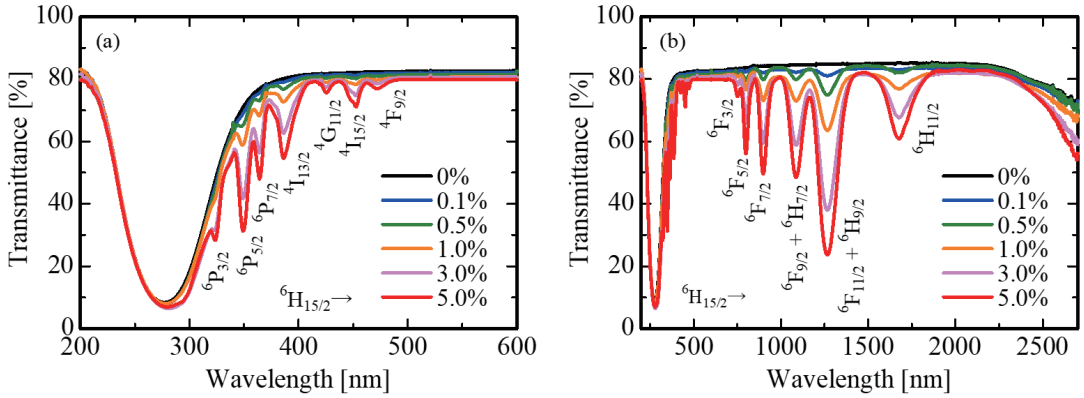

Fig. 3. (Color online) In-line transmittance spectra at (a) 200–600 and (b) 200–2700 nm.

Figure 4 shows the PL emission and excitation contour graph of the undoped and 0.5% Dy-doped glasses as representative examples. The Dy-doped glasses excited at 300–500 nm showed emission lines at 480, 570, 660, and 750 nm due to the electron transitions of $^4F_{9/2} \rightarrow {}^6H_{15/2}$, $^6H_{13/2}$, $^6H_{11/2}$, and $^6H_{9/2}$, respectively.[25,26] The PL *QY*s obtained upon 390 nm excitation were 19.8% (0.1% Dy), 34.8% (0.5% Dy), 20.5% (1.0% Dy), 4.5% (3.0% Dy), and 1.4% (5.0% Dy). The 0.5% Dy-doped glass showed the maximum PL *QY*, and concentration quenching was observed at Dy concentrations from 0.5 to 5.0%. Figure 5 shows PL decay curves of the Dy-doped glasses monitored at 570 nm upon 340–390 nm excitation. The PL decay curve of the 0.1% Dy-doped samples could be approximated to an exponential decay function, and the other decay curves were reproduced by a sum of two exponential decay functions. The obtained PL decay time constants (millisecond order) were typical for 4f-4f transitions of Dy^{3+}.[27,28] The two components in the PL decay curves may arise from the energy transfer between Dy^{3+} ions because the number of neighboring Dy^{3+} ions increases with Dy concentration.[29,30]

Figure 6 shows TSL glow curves of the undoped and Dy-doped glasses after 1 Gy X-ray irradiation. A broad glow peak was observed at ~75 °C in the Dy-doped samples, while the undoped sample showed no glow peak. The peak position shifted to a higher temperature

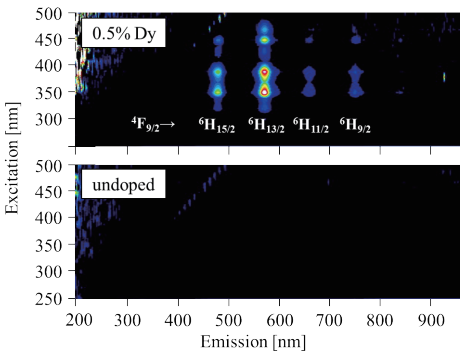

Fig. 4. (Color online) PL emission and excitation contour graph.

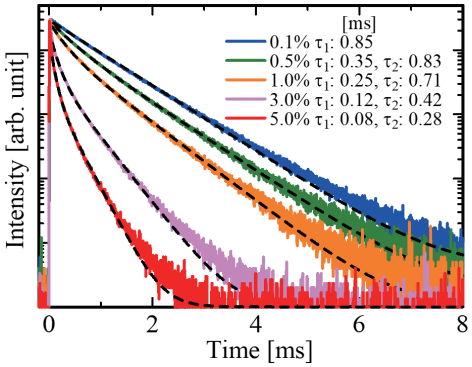

Fig. 5. (Color online) PL decay time profiles under 340–390 nm excitation.

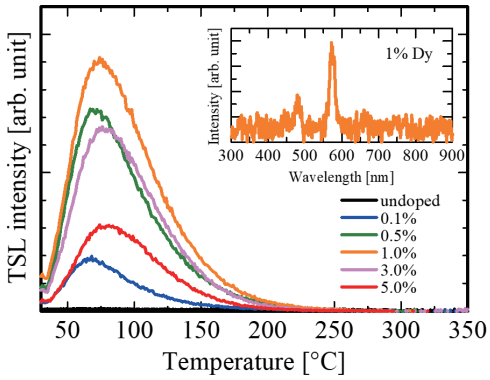

Fig. 6. (Color online) TSL glow curves and TSL spectrum.

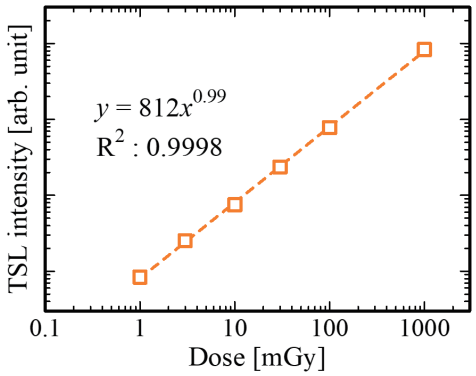

Fig. 7. (Color online) TSL dose response function of the 1.0% Dy-doped sample.

side with increasing Dy concentration. The discrepancy in the peak temperature of the Dy-doped samples was considered attributable to the change in the structural defect density of the Li_2O–B_2O_3 glass caused by the addition of Dy. The highest TSL intensity was obtained in the 1.0% Dy-doped glass, and the Dy concentration dependence of the TSL intensity was different from those of the PL *QY*s. Two possible explanations exist: the increase in Z_{eff} and the enhancement of transport efficiency by Dy doping. The Z_{eff} of the glass samples was increased by Dy doping, and the actual absorbed dose would increase, resulting in the increase in the density of electrons generated by radiation. Moreover, the numbers of trapping and luminescence centers changed according to Dy concentration, and the transport efficiency of electrons generated by radiation would be enhanced. The inset of Fig. 6 depicts the TSL spectrum of the 1.0% Dy-doped glass after X-ray irradiation under heating at 75 °C. The TSL spectrum had two peaks at 470 and 570 nm. Similarly to the PL spectra, these peaks originated from 4f-4f transitions of Dy^{3+}.[31,32] It was determined throughout this experiment that the TSL emission origin was Dy^{3+}. Regarding the characteristics of the device, Fig. 7 indicates the TSL dose response of the 1.0% Dy-doped glass as a representative. The tested dose range was 1–1000 mGy. The 1.0% Dy-doped sample showed a linear response in the range of 1–1000 mGy.

4. Conclusions

Li_2O–B_2O_3 glasses doped with 0.1, 0.5, 1.0, 3.0, and 5.0% Dy were synthesized by the melt-quenching method. Undoped and Dy-doped Li_2O–B_2O_3 glasses were visibly transparent, and the highest PL *QY* was ~35% for the 0.5% Dy-doped glass. The 480 and 570 nm emission peaks were observed in both the PL and TSL spectra, and the PL decay time constants were in millisecond order. The intense glow peak was detected at approximately 75 °C in the TSL glow curves. Among the current samples, the 1.0% Dy-doped Li_2O–B_2O_3 glass had the best TSL intensity and functioned as a dosimetric material in the dose range of 1–1000 mGy.

Acknowledgments

This work was supported by MEXT Grants-in-Aid for Scientific Research A (22H00309), Scientific Research B (21H03736, 22H03872, and 24K03197), Exploratory Research (22K18997), and Early-Career Scientists (23K13689), and Nippon Sheet Glass Foundation, Terumo Life Science Foundation, KRF Foundation, Tokuyama Science Foundation, Iketani Science and Technology Foundation, Iwatani Naoji Foundation, and Foundation for Nara Institute of Science and Technology.

References

1 M. Koshimizu, K. Oba, Y. Fujimoto, and K. Asai: Sens. Mater. **36** (2024) 565. https://doi.org/10.18494/SAM4761
2 R. Tsubouchi, H. Fukushima, T. Kato, D. Nakauchi, S. Saijo, T. Matsuura, N. Kawaguchi, T. Yoneda, and T. Yanagida: Sens. Mater. **36** (2024) 481. https://doi.org/10.18494/SAM4763
3 T. Kato, D. Nakauchi, N. Kawaguchi, and T. Yanagida: Jpn. J. Appl. Phys. **62** (2023) 010604. https://doi.org/10.35848/1347-4065/ac94ff
4 T. Kato, H. Kimura, K. Okazaki, D. Nakauchi, N. Kawaguchi, and T. Yanagida: Sens. Mater. **35** (2023) 483. https://doi.org/10.18494/SAM4137
5 S. Otake, H. Sakaguchi, Y. Yoshikawa, T. Kato, D. Nakauchi, N. Kawaguchi, and T. Yanagida: Sens. Mater. **36** (2024) 539. https://doi.org/10.18494/SAM4759
6 H. Nanto and G. Okada: Jpn. J. Appl. Phys. **62** (2023) 010505. https://doi.org/10.35848/1347-4065/ac9106
7 H. Kawamoto, Y. Fujimoto, and K. Asai: Sens. Mater. **36** (2024) 607. https://doi.org/10.18494/SAM4766
8 H. Ito, G. Okada, Y. Koguchi, W. Kada, K. Watanabe, and H. Nanto: Sens. Mater. **36** (2024) 559. https://doi.org/10.18494/SAM4765
9 H. Kawamoto, M. Koshimizu, Y. Fujimoto, and K. Asai: Jpn. J. Appl. Phys. **62** (2023) 010501. https://doi.org/10.35848/1347-4065/ac9cb0
10 V. E. Kafadar, R. G. Yildirim, H. Zebari, and D. Zebari: Thermochim. Acta **575** (2014) 300. https://doi.org/10.1016/j.tca.2013.11.017
11 M. Danilkin, I. Jaek, M. Kerikmäe, A. Lust, H. Mändar, L. Pung, A. Ratas, V. Seeman, S. Klimonsky, and V. Kuznetsov: Radiat. Meas. **45** (2010) 562. https://doi.org/10.1016/j.radmeas.2010.01.045
12 V. M. Holovey, V. I. Lyamayev, A. M. Solomon, N. N. Birov, P. P. Puga, and V. T. Maslyuk: Inorg. Mater. **42** (2006) 1265. https://doi.org/10.1134/S0020168506110161
13 A. Kelemen, V. Holovey, and M. Ignatovych: Radiat. Meas. **43** (2008) 375. https://doi.org/10.1016/j.radmeas.2007.11.083
14 V. M. Holovey, K. P. Popovich, D. B. Goyer, V. M. Krasylynets, and A. V. Gomonnai: Radiat. Eff. Defects Solids **166** (2011) 522. https://doi.org/10.1080/10420150.2011.559235
15 H. S. Hafez, A. M. Moanes, M. M. Alokr, and H. M. Essa: Arab J. Nucl. Sci. Appl. **49** (2016) 1.
16 B. T. Huy, V. X. Quang, and H. T. B. Chau: J. Lumin. **128** (2008) 1601. https://doi.org/10.1016/j.jlumin.2008.03.007

17 E. Pekpak, A. Yilmaz, and G. Ozbayoglu: The Open Mineral Processing J. **3** (2014) 14. https://doi.org/10.2174/1874841401003010014
18 L. Reddy: J. Fluoresc. **33** (2023) 2181. https://doi.org/10.1007/s10895-023-03250-y
19 A. Necmeddin Yazici, R. Chen, S. Solak, and Z. Yegingil: J. Phys. D: Appl. Phys. **35** (2002) 2526. https://doi.org/10.1088/0022-3727/35/20/311
20 G. Okada, T. Kato, D. Nakauchi, K. Fukuda, and T. Yanagida: Sens. Mater. **28** (2016) 897. https://doi.org/10.18494/SAM.2016.1357
21 T. Kato, G. Okada, N. Kawaguchi, H. Masai, and T. Yanagida: J. Non-Cryst. Solids **501** (2018) 116. https://doi.org/10.1016/j.jnoncrysol.2018.01.021
22 H. Samizo, T. Kato, N. Kawano, G. Okada, N. Kawaguchi, and T. Yanagida: J. Mater. Sci.: Mater. Electron. **29** (2018) 1985. https://doi.org/10.1007/s10854-017-8109-6
23 R. Lohan, A. Kumar, M. K. Sahu, A. Mor, V. Kumar, N. Deopa, and A. S. Rao: J. Mater. Sci.: Mater. Electron. **34** (2023) 1. https://doi.org/10.1007/s10854-023-10055-z
24 M. V. Rao, B. Shanmugavelu, and V. V. R. K. Kumar: J. Lumin. **181** (2017) 291. https://doi.org/10.1016/j.jlumin.2016.09.012
25 X. Y. Sun, S. Wu, X. Liu, P. Gao, and S. M. Huang: J. Non-Cryst. Solids **368** (2013) 51. https://doi.org/10.1016/j.jnoncrysol.2013.03.004
26 A. C. Rimbach, F. Steudel, B. Ahrens, and S. Schweizer: Phys. Chem. Glasses **59** (2018) 93. https://doi.org/10.13036/17533562.59.2.027
27 S. Chemingui, M. Ferhi, K. Horchani-Naifer, and M. Férid: J. Lumin. **166** (2015) 82. https://doi.org/10.1016/j.jlumin.2015.05.018
28 J. Sun, X. Zhang, Z. Xia, and H. Du: Mater. Res. Bull. **46** (2011) 2179. https://doi.org/10.1016/j.materresbull.2011.07.033
29 V. Uma, K. Marimuthu, and G. Muralidharan: J. Fluoresc. **26** (2016) 2281. https://doi.org/10.1007/s10895-016-1924-y
30 V. B. Sreedhar, D. Ramachari, and C. K. Jayasankar: Physica B **408** (2013) 158. https://doi.org/10.1016/j.physb.2012.09.047
31 T. Kato, D. Nakauchi, N. Kawaguchi, and T. Yanagida: Optik **207** (2020) 164433. https://doi.org/10.1016/j.ijleo.2020.164433
32 T. Kato, D. Nakauchi, N. Kawaguchi, and T. Yanagida: Opt. Mater. **132** (2022) 112785. https://doi.org/10.1016/j.optmat.2022.112785